RESIN FLOW FRONT MONITORING FOR VARTM USING FIBER BRAGG GRATINGS

Soohyun Eum*, Kazuro Kageyama*, Hideaki Murayama*, Kiyoshi Uzawa*, Isamu Ohsawa*, Makoto Kanai*, Hirotaka Igawa**

***Department of Environmental and Ocean Engineering, The University of Tokyo, 7-3-1, Hongo, Bunkyo-ku, Tokyo, Japan, 113-8656 Japan**

**** Japan Aerospace Exploration Agency, 6-13-1 Osawa, Mitaka-shi, Tokyo, 181-0015 Japan**

Keywords: *Resin flow front monitoring, VARTM, FBG, WDM, OFDR*

Abstract

In this study, we implemented resin flow front monitoring by using fiber Bragg gratings (FBGs) during vacuum assisted resin transfer molding (VARTM). We employed wavelength division multiplexing (WDM) technique and optical frequency domain reflectometry (OFDR) to monitor resin flow front. FBGs were embedded in the glass fiber preform. During VARTM, the embedded FBGs could measure how the preform affected the sensor with vacuum pressure and resin was flowed into the preform. In this study, we intended to detect the gradient of compressive strain between impregnated part and unimpregnated one within FBG. We could get the wavelength shift due to the change of compressive strain along gauge length of FBG. Therefore, we could know the resin flow front with the gradient of compressive strain of FBG.

1 Introduction

Vacuum assisted resin transfer molding (VARTM) process is one of liquid composite molding processes to manufacture light weight composite structures with good quality and at a low cost. VARTM is widely used in aerospace, automobile, shipbuilding and various industry fields for its advantages. VARTM can not only save tooling cost but also manufacture large structures [1,2] in comparison with traditional resin transfer molding (RTM) or autoclave molding because VARTM can produce the composite structure with one-side tool and lower curing temperature and pressure.

In VARMT, the preform is laid on a one-side tool. The porous resin distribute medium is located on the preform to enhance the flow of resin, and this assembly is bagged with vacuum bag film. Vacuum is applied to remove air bubbles including in resin, induce high fiber volume content and draws resin into the preform. After the resin filling is complete, the resin is cured with keeping compaction of the preform at room temperature.

Resin flow condition is important during the resin infusion process. As the structures become lager or thicker, or the preform with low permeability is adapted, the possibility of dry spot formation will be increased during resin infusion [3] and resin may not saturate the preform perfectly. During the curing process, the shrinkage of thermosetting resin causes residual stress and lower dimensional stability. Therefore resin flow condition and cure monitoring are required to guarantee or improve the quality of the composite structure manufactured by VARTM.

Some researches have studied to monitor resin flow front and/or resin cure for VARTM using optical fiber sensors. For example, when the uncoated optical fiber is surrounded by resin, the resin will change its color according to cure. Resin flow and cure condition can be monitored by the change of the transmission spectrum or the optical power output due to the refractive index changes of the surrounding resin [4-7]. Direct current resistance measurement using the SMARTweave system has been employed to monitor resin position and cure state as the sensing gap between two crossing conductive filaments is filled with resin [8-11]. By using ultrasonic transmission, the resin propagation can be detected [12-13]. However the research about structural health monitoring with the same sensor for

process monitoring is not conducted yet. If different types of sensor are used by the monitoring objects in VARTM, the sensing system will be expensive and complicated.

To monitor structural conditions, optical fiber sensors have been adapted in recent years because they can be embedded easily into composites because of their flexibility and thin diameter and they can apply to CFRP because of withstand voltage and anti-electromagnetic induction. In this study, fiber Bragg grating (FBG) was adopted as optical fiber sensor to implement effectively process and structural health monitoring of composite structures manufactured by VARTM.

In the previous study [14], we found that when the preform was still dry, FBG measured the strain developments due to the movement of the glass fiber tow of the preform under the vacuum pressure. We also found that the strain was released after FBG had been wetted during the resin infusion process. We assumed that FBG can monitor the resin flow front according to measure the strain changes and then FBG can also evaluate resin cure and in-service inspection of composite structures.

In the case of the resin flow front monitoring of the large scale composite structure, the quasi-distributed sensing is required to monitor the entire resin flow front with the short gauge FBGs. At the particular part, for example, the stress concentration part and the part which has a large curvature or a low permeability, the distributed sensing with the high spatial resolution is required to acquire more detail information at such parts.

In this study, we investigate the capability of the resin flow front monitoring due to the strain change detected by FBGs embedded in the preform. The resin flow front monitoring according to the quasi-distributed sensing and the distributed sensing was implemented. Wavelength division multiplexing (WDM) method was employed for the quasi-distributed sensing. Optical frequency domain reflectometry (OFDR) was chosen for the distributed measurement with the high spatial resolution which is less than 1 *mm*. We could detect the resin flow front as well as the progress of the resin infusion process, such as starting the vacuum pump, by monitoring the strain data obtained from either the quasi-distributed or distributed sensing system.

2 Sensing systems and Experimental method

2.1 Fiber Bragg Grating (FBG)

Fiber Bragg Grating (FBG) [15] is a periodic perturbation of the reflective index and consists of a single mode fiber that has photo-inscribed gratings into a silica core. When the broadband light propagates through the fiber core, the narrowband spectrum well defined peak is reflected back with the Bragg wavelength. A notched spectrum is transmitted through FBG. The Bragg wavelength is defined as

$$\lambda_B = 2n_{eff}\Lambda \tag{1}$$

where the Bragg wavelength (λ_B) is the center wavelength of the reflected light, n_{eff} is the effective index of refraction of the fiber core and Λ is the period of the grating. An applied strain to the FBG is expressed by the Bragg wavelength shift, $\Delta\lambda_B$, as following [16]

$$\Delta\varepsilon = \frac{\Delta\lambda_B}{0.78\times10^{-6}\cdot\lambda_B}. \tag{2}$$

In this study, a long gauge FBG whose gauge length is about 100 *mm* and an ordinary one whose gauge length is 10 *mm* were employed for the resin flow front monitoring based on OFDR and optical spectrum meter, respectively.

2.2 Quasi-distributed sensing system with FBGs

WDM technique provides the quasi-distributed sensing because tens of FBGs can be multiplexed along a single fiber [16]. Fig. 1 shows the set up of the sensing system based on WDM technique. This system used in this study can measure strain or temperature with high speed and high accuracy. It consists of FBG sensor monitor (Yokogawa FB 200), ASE light source, an optical circulator and FBGs. Broadband lights from the ASE light source are illuminated to FBG through the optical circulator. The reflected FBG spectra are sent to the FBG sensor monitor through the optical circulator. The center wavelength for each FBG is outputted from the reflected FBG spectra.

The data acquisition/processing program were written in LabVIEW. The data acquisition and the control of the sensing system were conducted through USB by personal computer. Table 1 describes the details of this system.

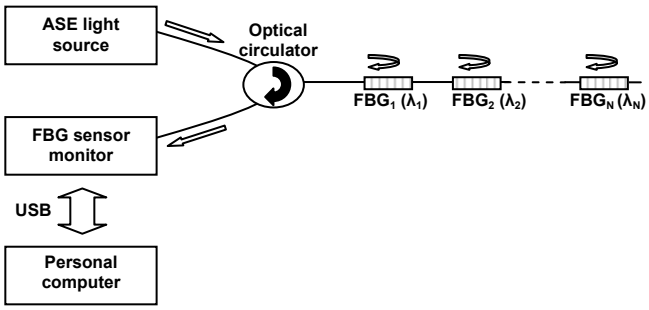

Fig. 1. The set up of quasi-distributed sensing system with a FBG array based on WDM technique

Table 1. Specification of the quasi-distributed sensing system

Item	Spec.
Number of FBG	~ 40
Measurement wavelength range	1527 ~ 1567 nm (40 nm)
Resolution	1 pm
Measurement power range	-4 dm ~ -65dm
Measurement cycle	10 ~ 990 ms

2.3 Distributed sensing system with long-gauge FBG

Distributed sensing system based on OFDR is consisted of wavelength tunable laser (ANDO AQ4321), two photodiode detectors (D1, D2), three broadband reflectors (R1, R2 and R3), three 3dB couplers (C1, C2 and C3), a long gauge FBG, personal computer and A/D converter (National Instrument PCI 6115) as shown in Fig. 2. The layout of this system is similar to the one reported by B.A. Childers et al [17]. The wavelength tunable laser is controlled with personal computer through GPIB, and a measured data is acquired by A/D converter. The light reflected between R3 and each grating is acquired by D2. The signal at D2 is given by

$$D_2 = \sum_i R_i \cos\left(k 2 n L_i\right), \tag{3}$$

where R_i is the spectrum of the i th grating, L_i is the path difference of the corresponding i th interferometer and k is the wavenumber of the light and is related to the wavelength λ and is given by the following equation.

$$k = \frac{2\pi}{\lambda} \tag{4}$$

The spectra of reflected light along the long gauge FBG can be determined by Fourier analysis [18, 19]. The details of signal process were written in Ref. 18 and 19.

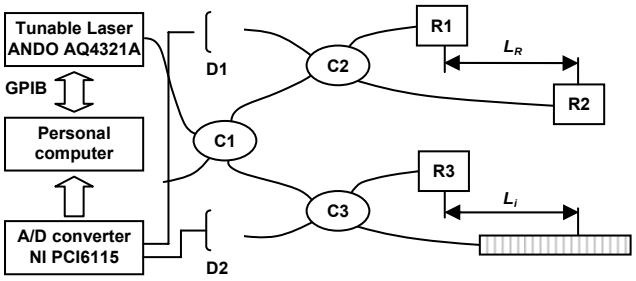

Fig. 2. Measurement system based on OFDR

2.4 Resin flow front monitoring during VARTM

Prior to monitor the resin flow front monitoring, the strain changes were measure at top, middle and bottom layers on the preforms (2, 4, 6, 10 and 20 plies of glass fabric) by FBG under the vacuum pressure.

In the case of the monitoring experiments by the quasi-distributed sensing system based on WDM technique, three FBGs on a single fiber were embedded on bottom, middle and top side layers on each preform with 10 *mm* interval each other as described in Table 2 and Fig 3 (a).

In the case of the monitoring experiments by the distributed sensing system based on OFDR, the long gauge FBG was located on the middle layer of the preform of 20 ply as shown in Fig. 3 (b).

The preform size was 400 *mm* $\times$ 100 *mm*. To prevent optical fiber from breaking by vacuum pressure, two acryl plates were installed at both edges of the preform. Tubes passed through the acryl plates, and each optical fiber was carried through each tube. The tool was enveloped by a vacuum bagging film, and then vacuum was applied to draw resin into the mold cavity. In this study, we used silicon oil which has similar viscosity with resin in order to reuse FBGs. The data was acquired at the intervals of 0.5 *s* and 1.4 *s* for the quasi-distributed sensing based on WDM technique and the distributed sensing based on OFDR, respectively.

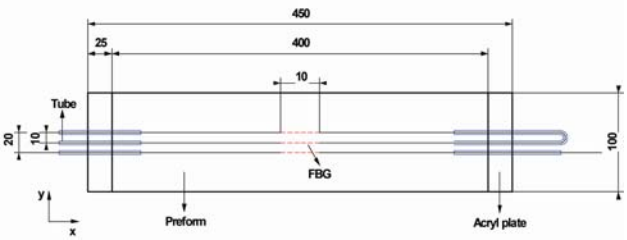

(a) FBG locations on the preform for optical spectrum meter measurement (unit: *mm*)

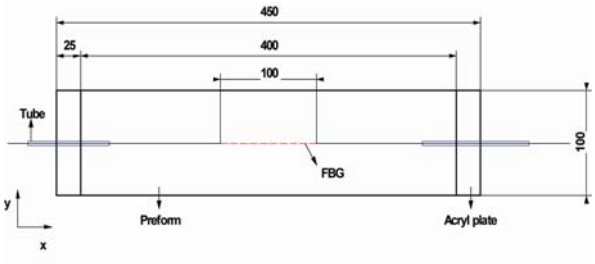

(b) Long gauge FBG location on the preform for OFDR measurement (unit: *mm*)

Fig. 3. Specimen for resin flow monitoring

Table 2. Experimental conditions

Sensing system	Preform	FBG location / Center wavelength [nm] 1550	1552	1557.5	1563.5	FBG gauge length
WDM	2 Ply	-	-	-	middle	10 mm
	4 Ply	-	1st layer	middle layer	3rd layer	
	6 Ply	-	1st layer	middle layer	5th layer	
	10 Ply	-	1st layer	middle layer	9th layer	
	20 Ply	-	1st layer	middle layer	19th layer	
OFDR	20 Ply	middle layer	-	-	-	100 mm

3 Results and discussions

3.1 The strain changes on the preform

Fig. 4 shows the responses of FBG embedded in the glass fiber preform under the vacuum pressure. The glass fiber tow of the 1st layer on the preform is difficult to move due to restriction of the tool surface under the vacuum pressure. In the cases of 2 ply and the 1st layer of the preform of 4 ply, the tensile strains were shown from the 2nd and 3rd layers of the preform of 4 ply, the compressive strains were developed by the movement of the glass fiber tow. As the preforms were thicker, the compressive strains on FBG were higher according to the movement of the glass fiber tow. In the same ply of the preform, the compressive strain on the middle layer was higher than the one on the both other layers. However, as the preform was thicker, the compressive strains between on middle and on top layer showed similar values.

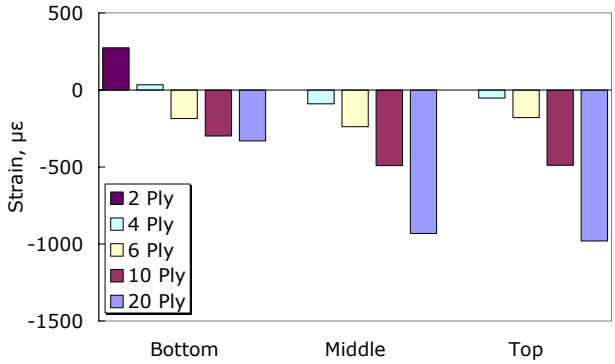

Fig. 4. The strain changes on each preform under the vacuum pressure

3.2 Resin flow front monitoring by the quasi-distributed sensing with FBGs

Fig. 5 shows the result of resin flow front monitoring on 2 ply of the preform. This plot well maps the strain changes during resin infusion process. When the vacuum pump was driven, the tensile strain was developed. Then, the tensile strain was decreased by the movement of the glass fiber tow of the preform. As the silicon oil toward FBG, the strain was rapidly decreased. When the silicon oil reached FBG, the gradient of compressive strain was decreased due to the release by the silicon oil. When the vacuum and resin ports were closed, the compressive strain was released by the redistribution of the pressure in vacuum bag. Approximately -40 $\mu\varepsilon$ was kept after close both ports. In this figure, we could know that the resin flow front was the inflexion point (245 *s*) of the compressive strain.

The strain changes on the top, middle and bottom layers of the preform of 4 ply during resin infusion process were plotted in Fig. 6. The compressive strains were developed on the 2nd and 3rd plies, while the tensile strain was developed on 1st layer under the vacuum pressure. When the resin port was opened, the strain was decreasing gradually until resin reached at FBG. When FBG was immerged by the silicon oil (458 *s*), the gradient of compressive strain on each layer was decreased by release of the vacuum pressure due to the silicon oil. The highest release of compressive strain was shown on the middle layer.

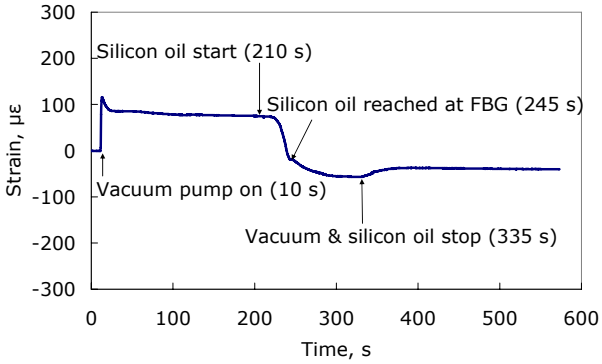

Fig. 5. Resin flow monitoring on 2 ply of the preform

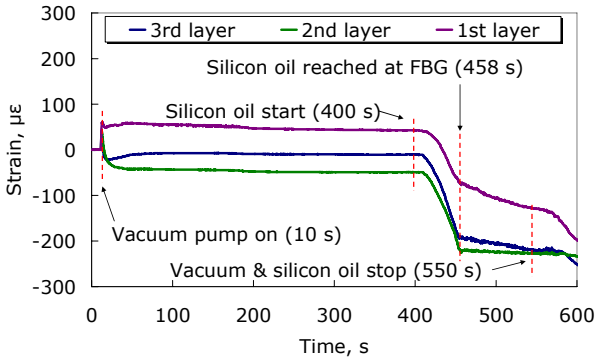

Fig. 6. Resin flow monitoring on 4 ply of the preform

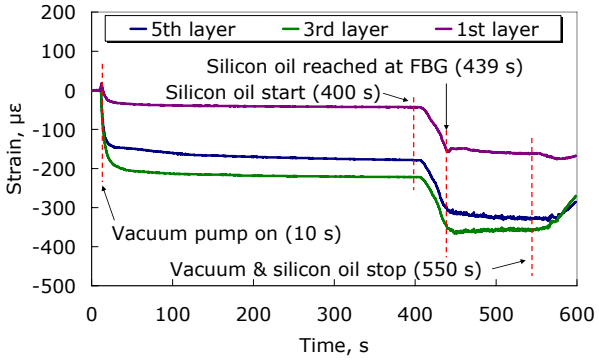

Fig. 7. Resin flow monitoring on 6 ply of the preform

Fig. 8 shows the strain changes on the preform of 10 ply. The similar rate of strain changes on each layer was also shown on this preform until resin reached at FBG. When the resin reached at FBG (450 *s*), the compressive strains on 1st and 9th layers were kept constantly and the reduction of compressive strain showed at the 5th layer noticeably by the release of the vacuum pressure.

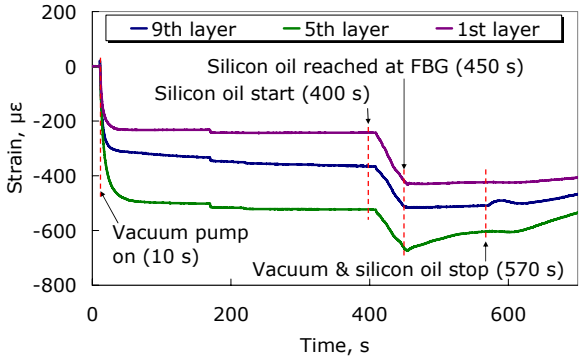

Fig. 8. Resin flow monitoring on 10 ply of the preform

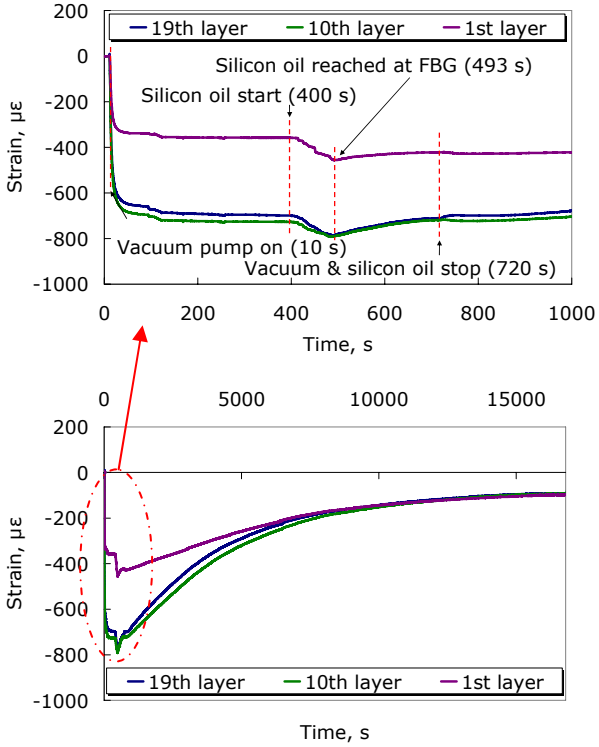

Fig. 9. Resin flow monitoring on 20 ply of the preform

Fig. 7 demonstrates the strain changes on each layer on the preform of 6 ply. On this preform, the compressive strain was developed on each layer under the vacuum pressure. From the preform of 6 ply, the strains changed steady on every layers during resin infusion process. Although the compressive strain values were different at an initial step, the later rates of strain change were similar each other. When the resin reached at FBG (439 *s*), the reduction of compressive strain was shown on the 3rd layer by the release of the vacuum pressure.

Fig. 9 shows the results of resin flow front monitoring. When the resin reached at FBG (493 *s*),

the reduction of compressive strain was shown on each layer by the release of the vacuum pressure. As the preform was thicker, the reduction of compressive strain was evident. After the both ports were closed, the compressive strain of approximately 100 $\mu\varepsilon$ was kept from approximately 15000 s.

From these results, we could monitor the whole progresses during the resin infusion process by the detected strain changes when the vacuum pump was driven and the resin port was opened and the both ports were closed as well as resin flow front. At the middle layers on each preform, the highest release of the compressive strain was shown. We could monitor the resin flow front at various layers on each preform by the release of the compressive strain.

3.3 Resin flow front monitoring by the distributed sensing with long guage FBG

The resin flow front monitoring was also conducted by using OFDR. In order to derive the wavelength shifts due to strain changes which were developed during VARTM process, the former wavelength distribution data has to be subtracted because the wavelength distribution is changed at all times during resin infusion process. Fig. 10 explains why the wavelength distribution data before 7 seconds has to be subtracted to derive the resin flow front. The plots show the distributed compressive strain during resin infusion process. The resin flow front is the gradient section of the compressive strain. The dashed line in this figure will be 0 as subtracting i-n th (n = 1, 2, 3,···) wavelength distribution data from i th one. Therefore, 0 point will be the resin flow front. The change of wavelength distribution due to subtracting i-5 th from i th is most optimal to recognize the resin flow front. In this study, the temperatures between the silicon oil and preform were same. Therefore, the change of temperature was zero ($C_T\Delta T_i=0$). The wavelength changes were affected by the changes of mechanical strain:

$$\Delta\lambda_i = \lambda_i - \lambda_{i-5} = C_\varepsilon \Delta\varepsilon_i + C_T \Delta T_i . \qquad (5)$$

The photoelastic coefficient of strain of the long gauge FBG, C_ε, was 0.0012 $nm/\mu\varepsilon$ (λ_B: 1550 nm) [16].

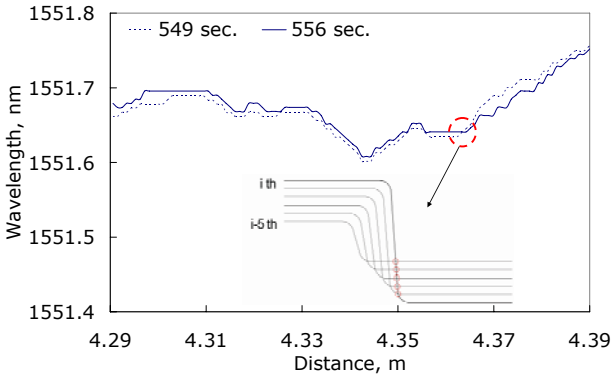

Fig. 10. Principle to derive the resin flow front

Fig. 11 shows the results of resin flow front monitoring acquired by OFDR and long gauge FBG at 1.4 s intervals during VARTM. The results demonstrate the movement of the resin from the resin inlet port to the vacuum port resulting in the strain distribution changes derived by subtracting the strain distribution before 7 seconds. The results were compared to the captured photos by the video camera. The video camera recording and the acquisition of OFDR signal were synchronized. The long gauge FBG of 100 mm was located at 4.29 m from R3 along the optical fiber.

When the silicon oil was not reached at FBG, the compressive strain of approximately 10 $\mu\varepsilon$ developed along whole gauge length of FBG compare to the 7 seconds former data as shown in Fig. 11 (a). As the silicon oil surrounded FBG, the compressive strain was released as shown in Fig. 11 (b). Therefore, the strain gradient was developed between the impregnated and unimpregnated preform. The threshold is 0 $\mu\varepsilon$. According to the silicon oil progress, the strain gradient also progressed as shown in Fig. 11 (b) ~ (d). The location of impregnated preform in the photos and the strain gradients shows good agreement. Approximately 10 $\mu\varepsilon$ of the compressive strain was released within the gauge length of FBG embedded in the impregnated preform and was developed within the gauge length of FBG embedded in the unimpregnated preform. It can be seen that the strain of 5 $\mu\varepsilon$ was released when the silicon oil surrounded whole gauge length of FBG compare to the 7 seconds former data as shown in Fig. 11 (d). These graphs show a filing time of approximately 54.6 s within 100 mm at the middle of the preform.

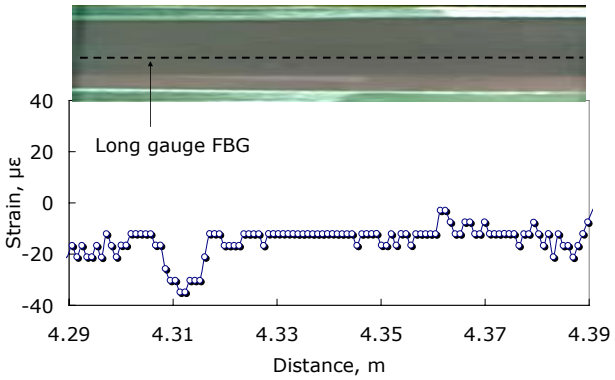

(a) Sampling No. 371 (519.4 *s*)

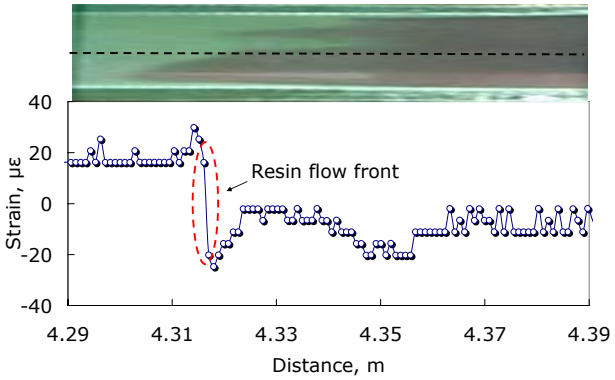

(b) Sampling No. 385 (539 *s*)

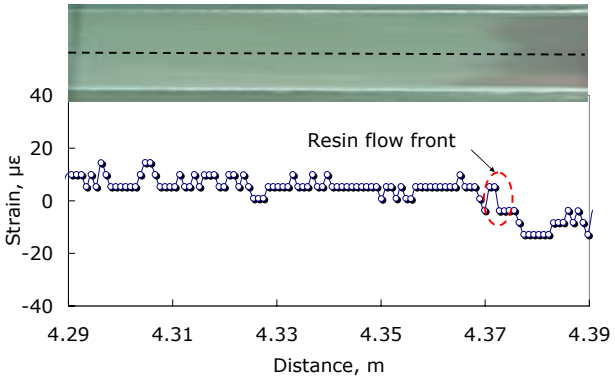

(c) Sampling No. 401 (561.4 *s*)

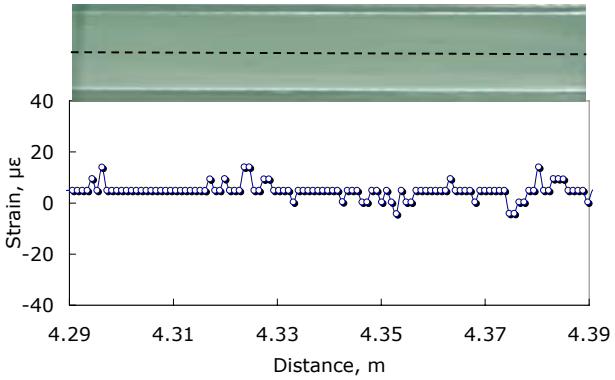

(d) Sampling No. 410 (574 *s*)

Fig. 11. Results of resin flow front monitoring acquired by OFDR and long gauge FBG

Fig. 12 shows the strain changes at 4.29 *m*, and 4.38 *m* during the silicon oil infusion process. The strain distribution under vacuum pressure when 504 *s* (Sampling No. 360 × 1.4 *s*) elapsed was subtracted from each acquired strain distribution from the inlet port was opened. The compressive strains were more developed until resin reached FBG. When resin reached FBG, the compressive strains were released by the impregnated resin on preform. In this figure, we could know that the times which resin reached at 4.29 *m* and 4.38 *m* were 521 *s* and 567 *s* approximately. It can be seen that the compressive strain was released by the silicon oil certainly in this figure.

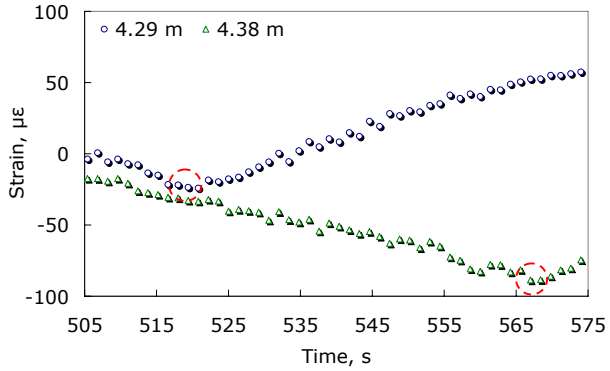

Fig. 12. Strain change at each position during resin infusion

4 Conclusions

In this study, the ability of resin flow front monitoring VARTM was investigated by using FBGs based on WDM technique and OFDR. We could monitor resin flow front by measuring the strain change during resin infusion process by using both sensing systems. In the case of WDM technique, we could monitor resin flow front on various layers on the preforms which had different ply. On the thicker preform, we could know the evident resin flow front monitoring as well as the whole progress during resin infusion process using the strain change. We could monitor the distributed resin flow front along the gauge length of FBG by using OFDR. We suggest the quasi-distributed sensing and the distributed sensing based on FBG to monitor the resin flow front. In the case of the entire resin flow front monitoring, the quasi-distributed sensing is acceptable while the distributed sensing is suitable for the particular part which has to a stress concentration, a large curvature or a low permeability. Accordingly, it is expected that the quality of the composite structures manufactured by

VARTM can be assured and controlled by the suggested systems in this study.

In future, we will try to clarify the mechanism of the strain change detected by FBG on the preform. Then, we will conduct the resin flow front monitoring with either the quasi-distributed or distributed sensing system on the large scale composite structure.

Acknowledgement

The author, Soohyun Eum, appreciates the support by the 21th Century COE Program, "Mechanical Systems Innovation and by the Korea Science and Engineering Foundation Grant funded by the Korea government (MOST)". The authors thank to Lazoc, Inc. who supported the quasi-distributed sensing system.

References

[1] J. Dai, D. Pellaton, and H.T. Hahn, "A comparative study of vacuum-assisted resin transfer molding (VARTM) for sandwich panels", *Polymer composites* Vol. 24, **No.** 6, pp.672-685, 2003

[2] W.D. Brouwer, E.C.F.C. van Herpt, M. Labordus, "Vacuum injection moulding for large structural application", *Composites: Part A* Vol, 34, pp. 551-558, 2003

[3] D. Bender, J. Schuster, D. Heider, "Flow rate control during vacuum-assisted resin transfer molding (VARTM) processing", *Compos Sci Technol*, Vol. 66, pp 2265-2271, 2006.

[4] Dara L. Woerdeman , Julie K. Spoerre, Kathleen M. Flynn and Richard S. Parnas, "Cure monitoring of the liquid composite molding process using fiber optic sensors", *Polymer composites*, Vol. 18, No. 1, pp. 133-150, 1997

[5] Youngki Yoon, Seunghwan Jeong, Wooil Lee, and Byungho Lee, "A Study on the measurement technique of resin flow and cure during the vacuum assisted resin transfer moulding process using the long period fiber bragg grating sensor", *Advanced composites letters,* Vol. 13, pp. 237-243, 2004

[6] C Doyle, A Martin, T Lui, M Wu, S Hayes, P A Crosby, C R Powell, D Brooks and G F Fernando, "In-situ process and condition monitoring of advanced fibre-reinfirced composite materials using optical fibre sensors", *Smart Materials and Structures,* Vol. 7, pp. 145-158, 1998

[7] Hyun-Kyu Kang, Dong-Hoon Kang, Hyung-Joon Bang, Chang-Sun Hong and Chun-Gon Kim, "Cure monitoring of composite laminates using fiber optic sensors", *Smart Materials and Structures* , Vol. 11, pp. 279-287, 2002

[8] Thierry Luthy and Paolo Ermanni, "Flow monitoring in liquid composite molding based on linear direct current sensing technique", *Polymer composites,* Vol. 24, No. 2, pp. 249-262, 2003

[9] Uday K Vaidya, Nitesh C Jadhav, Mahesh V Hosur, John W Gillespie and Bruce K Fink, "Assessment of flow and cure monitoring using direct current and alternating current sensing in vacuum-assisted resin transfer molding" *Smart Materials and Structures,* Vol. 9, pp. 727-736, 2000

[10] Kei Urabe, Tomonaga Okabe, Hiroshi Tsuda, "Monitoring of resin flow and cure with an electromagnetic wave transmission line using carbon fiber as conductive elements", *Composites Science and Technology,* Vol. 62, pp. 791-797, 2002

[11] T. Luthy, P. Ermanni, "Linear direct current sensing system for flow monitoring in liquid composite moulding", *Composites: Part A,* Vol. 33, pp. 385-397, 2002

[12] E. Schmachtenberg, J. Schulte zur Heide, J. Topker, "Application of ultrasonics for the process control of Resin Transfer Moulding (RTM)" *Polymer Testing,* Vol. 24, pp. 330-338, 2005

[13] T. Stoven, F. Weyrauch, P. Mitschang, M. Neitzel, "Continuous monitoring of three-dimensional resin flow through a fibre perform" *Composites : Part A,* Vol. 34, pp. 475-480, 2003

[14] S.H. Eum, K. Kageyama, H. Murayama, I. Ohsawa, K. Uzawa, and M. Kanai, "Application of Fiber Bragg Grating Distributed Sensors to Process and Health Monitoring of Composite Structures" *Proc. of 18th International optical fiber sensors,* ThD4, 2006

[15] Hiroshi Tsuda, Nobuyuki Toyama, KeiUrabe and Junji Takatsubo, "Impact damage detection in CFRP using fiber Bragg gratings", *Smart Materials and Structures,* Vol. 13, pp. 719–724, 2004

[16] Alan D. Kersey, Michael A. Davis, Heather J. Patrick, Michel LeBlanc, K.P. Koo, C.G. Askins, M.A. Putnam and E. Joseph Friebele, "Fiber Grating Sensors", *Journal of Lightwave Technology,* Vol. 15, pp. 1442-1463, 1997

[17] Brooks A. Childers, Mark E. Froggatt, Sideny G. Allison, Thomas C. Moore, Sr., David A. Hare, Christopher F. Batten, Dawn C. Jegley, "Use of 3000 Bragg grating strain sensors distributed on four eight-meter optical fibers during static load tests of a composite structure", *Proc. of SPIE*, Vol. 4332, pp.133-142, 2001

[18] Igawa H., Murayama H., Kasai T., Yamaguchi I., Kageyama K., Ohta K. "Measurements of strain distributions with a long gauge FBG sensor using optical frequency domain reflectometry", *Proc. of SPIE*, Vol. 5855, pp.547-550, 2005.

[19] H. Murayama, H. Igawa, K. Kageyama, K. Ohta, I. Ohsawa, K. Uzawa, M. Kanai, T. Kasai and I. Yamaguchi, "Distributed strain measurement with high spatial resolution using fiber bragg gratings and optical frequency domain reflectometry" *Proc. of 18th International optical fiber sensors,* ThE40, 2006